

Mass Spectral Determination of Fasting Tear Glucose Concentrations in Nondiabetic Volunteers, Justin T. Baca,¹ Christopher R. Taormina,¹ Eleanor Feingold,³ David N. Finegold,² Joseph J. Grabowski,¹ and Sanford A. Asher*¹ (¹Department of Chemistry, University of Pittsburgh, Pittsburgh, PA; ²Department of Pediatrics, University of Pittsburgh School of Medicine, Children's Hospital of Pittsburgh, Pittsburgh, PA; ³Department of Human Genetics and Department of Biostatistics, University of Pittsburgh Graduate School of Public Health, Pittsburgh, PA; * address correspondence to this author at: Department of Chemistry, Chevron Science Center, 219 Parkman Ave., Pittsburgh, PA 15260; fax 412-624-0588, e-mail asher@pitt.edu)

Background: There is considerable disagreement regarding the concentration of glucose in tears and its relationship to the concentration in blood. Improved sampling and analysis methods may resolve these discrepancies and possibly provide a basis for in situ tear glucose sensors.

Methods: We used liquid chromatography (LC) with electrospray ionization mass spectrometry (ESI-MS) to determine glucose in 1- μ L tear fluid samples obtained from 25 fasting study participants. Tear fluid was collected with microcapillaries and a slitlamp microscope.

Results: The median (range) of fasting tear glucose concentrations was 28 (7–161) μ mol/L or 0.50 (0.13–2.90) mg/dL. The SD of tear glucose measurements for individuals varied linearly with the mean tear glucose concentration and was approximately half of the mean. We found no significant difference in tear glucose concentrations between contact lens users and nonusers ($P = 0.715$). We observed significant correlations between fasting blood and tear glucose concentrations ($R = 0.50$, $P = 0.01$).

Conclusions: Our tear fluid collection and analysis method enables reliable measurement of equilibrium, fasting tear glucose concentrations. These concentrations are lower than those previously reported for nondiabetic persons. Larger population studies are required to determine correlations between blood and tear glucose concentrations and to determine the utility of contact lens-based sensors for the monitoring of diabetes. Our methods are applicable for study of other tear fluid analytes and may prove useful for monitoring other disease states.

© 2007 American Association for Clinical Chemistry

Glucose has been a recognized component of tear fluid since the early 1900s, but disagreement continues regarding its concentration in tear fluid and its correlation with blood glucose concentration (1–6). Literature reports of normal tear glucose concentrations range between 0 and 9.1 mmol/L (164 mg/dL), with median values of 110–280 μ mol/L (1.98 and 5.04 mg/dL) (1, 7). In a recent study of 121 persons, tear glucose concentrations ranged from

below the limit of detection to 9.1 mmol/L (164 mg/dL) (7). Much of the difference in reported tear glucose concentrations is likely from the use of different tear collection techniques (8). Collection techniques causing severe eye irritation [such as filter paper collection (6)] are associated with the highest tear glucose concentrations, whereas less irritating techniques (such as glass capillary collection) are associated with the lowest (2, 3). Chemically stimulated tears have increased tear glucose (8, 9). Reliable tear sampling may also be confounded by individual differences in tolerance to real or expected eye stimulation during sampling. (See the Data Supplement that accompanies the online version of this Technical Brief at <http://www.clinchem.org/content/vol53/issue7> for an extensive review of the tear glucose literature.)

Improved tear fluid collection, and the ability to analyze very low volumes of tear fluid, may dramatically improve measurement of tear fluid glucose concentrations and help resolve the reported discrepancies in basal tear glucose concentrations. Improved methods would also enable the study of physiologic glucose transport in the eye and advance the use of tear fluid as a surrogate for blood in measuring other clinically important analytes.

Some groups have tried to use tear glucose to diagnose diabetes (4, 5), and others have proposed continuous monitoring of blood glucose concentrations by use of contact lenses with glucose sensors (10–13). We recently reported a photonic crystal glucose-sensing material for noninvasive monitoring of glucose in tear fluid (10). Detailed understanding of tear glucose concentration and its regulation is critical to developing noninvasive glucose sensors.

We recently developed an electrospray ionization mass spectrometry (ESI-MS) method for measuring glucose in 1- μ L samples of collected tear fluid (9). With this method, we studied basal tear glucose concentrations in healthy persons without diabetes.

We recruited volunteers (age 18–60 years) within and around the University of Pittsburgh. Persons with a history of diabetes were excluded. Blood and tear samples were obtained after participants had fasted overnight for at least 8 h. The samples were always collected in the same order: capillary blood from the finger pad, tear fluid from the left eye, and then tear fluid from the right eye. This sequence was repeated 3 times for each study participant, with at least 10 min between successive blood sample collections. Glucose in capillary blood was measured with an Accu-Chek® Compact glucometer (Roche), according to the manufacturer's protocol.

A total of 26 volunteers completed the study; 11 wore their usual contact lenses at the time of the study, and 15 did not wear contact lenses. The type of contact lenses worn were daily disposable ($n = 1$), daily wear ($n = 6$), extended wear ($n = 1$), and silicone hydrogel lenses ($n = 2$). Of the 15 non-contact lens wearers, 1 had a history of contact lens use, but did not wear contacts on the day of

the study. For 1 contact lens wearer, the collected tear samples were lost because of vial breakage before analysis. For 2 participants (1 from the contact lens group and 1 from the non-contact lens group), 1 of the 6 tear glucose samples was lost because of instrument failure. The tear glucose concentration statistics for these 2 participants were determined from only 5 samples. The University of Pittsburgh School of Medicine Institutional Review Board approved all clinical procedures, and all participants signed a detailed informed consent form.

Tear fluid samples of 1 μL were collected and analyzed by liquid chromatography ESI-MS as previously reported (9). Three aliquots of each tear sample were injected into the analyzer to determine the mean glucose concentration. Our study found much lower tear fluid glucose concentrations for healthy individuals than did previous studies (see Fig. 1 in the online Data Supplement).

The population median (range) of the tear glucose concentrations were 28 (7–161) $\mu\text{mol/L}$ [0.50 (0.13–2.90) mg/dL]. The distribution of mean tear glucose concentrations was highly skewed; <28 $\mu\text{mol/L}$ (0.50 mg/dL) in 50% of the study participants and <42 $\mu\text{mol/L}$ (0.76 mg/dL) in 80% of the study participants. Two individuals were observed rubbing their eyes during the course of the study, and they had the highest mean (SD) tear glucose concentrations: 128 (75) and 161 (71) $\mu\text{mol/L}$ or 2.31 (1.35) and 2.90 (1.28) mg/dL.

Because the SD of the mean tear glucose concentration for each participant was proportional to the mean for each participant, a natural log transformation was applied to the tear glucose concentration values (see Figs. 2 and 3 in the online Data Supplement). After transformation, standard statistical methods were applied.

Contact lens use did not affect mean tear glucose ($P = 0.715$). Transformed tear glucose concentrations were significantly correlated with mean blood glucose ($R = 0.50$, $P = 0.01$, Fig. 1A). This correlation for fasting tear and blood glucose is similar to that reported by Daum and Hill of $R = 0.53$ for blood and tear glucose measurement variations throughout the day. However, they reported a mean (SD) population tear fluid glucose concentration of 420 (355) $\mu\text{mol/L}$ or 7.57 (6.40) mg/dL.

The glucose concentrations in the right and left eyes were highly correlated within individuals (Fig. 1B). There was no evidence that eye-to-eye variation in individual study participants differed significantly from variation in a single eye over time. Furthermore, we observed no evidence that variation in tear glucose concentration between individuals with similar blood glucose concentrations was greater than variation in tear glucose concentration within an individual.

The correlation between the transformed tear glucose value and the average blood glucose concentration appears to be stronger for non-contact lens wearers than for participants wearing contact lenses ($R = 0.70$ vs $R = 0.22$).

However, analysis of covariance does not indicate a significant difference ($P = 0.63$).

The ESI-MS method used here enables reliable determination of basal tear glucose concentrations in fasting individuals. Study participants had fasted overnight, and had stable blood glucose concentrations over the brief course of the study. We observed much lower basal tear glucose concentrations than previously reported for healthy individuals. This difference is likely a result of our sampling methods, which were less irritating than earlier methods that stimulated tear production chemically or with filter paper (8). If our collection method had caused significant irritation, we would have expected tear glucose concentrations to increase over the course of the

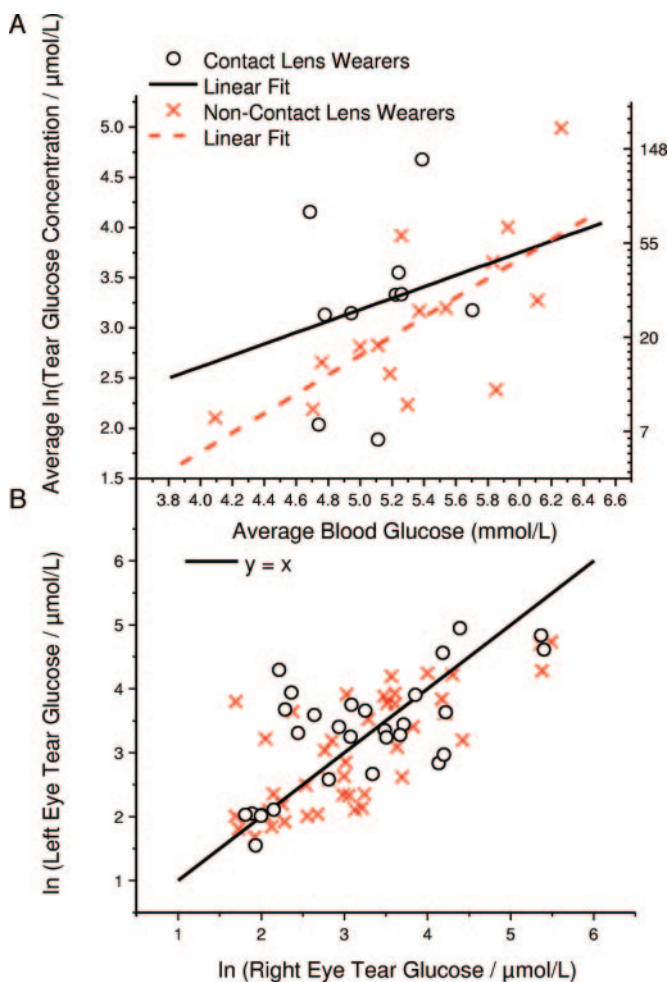


Fig. 1. (A) Correlation ($P = 0.01$) between the mean $\ln(\text{tear glucose concentration})$ and the mean blood glucose concentration.

A linear regression for all participants gives $y = 0.80x - 1.07$ ($R = 0.50$). Linear regression for the subpopulations of contact wearers and non-contact wearers gives $y = 0.570x + 0.332$ ($R = 0.22$) for contact lens wearers and $y = 0.961x - 2.079$ ($R = 0.70$) for non-contact wearers. (B), paired tear glucose observations within study participants. No significant differences were observed between right and left eyes ($P = 0.76$, two-tailed paired t -test), but results may differ at any given time. The left and right tear glucose determinations that are closest in time are plotted against each other. There are hence 3 data points for each study participant.

study. We observed no evidence of such an increase (see Fig. 4 in the online Data Supplement).

We observed significant variation in tear glucose concentrations between the 2 eyes of individual study participants, as well as over time within a single eye. During this study, we were cognizant of potential confounding events such as yawning and eye rubbing. Although the 2 individuals who rubbed their eyes during the study had the highest glucose concentrations, events like these do not explain the large within-individual differences observed.

Variations in tear glucose concentrations within a single individual must derive from the sum of the biological variance and any variances associated with sampling and measurement. The error in our tear fluid collection volumes was negligible (9); the SD observed for an individual was ~3 times the SD of the 3 replicate mass spectral measurements of a single tear fluid sample. The relative SDs of these 3 replicates varied somewhat with glucose concentration but had a median value of 14%. Thus, the observed SD in tear glucose measurements derive mainly from actual variations of the glucose concentration in the different tear fluid samples.

We did not observe a systematic increase over time in glucose concentration variations that could result from the effect of tear depletion during repeated measurements. Tear glucose concentration appeared to vary randomly over the repeated sampling events.

We observed variations in tear glucose concentrations among fasting individuals and a significant correlation between $\ln(\text{tear glucose concentration})$ and blood glucose concentration. Mean fasting tear glucose concentrations did not differ significantly in relation to contact lens use. Further studies are needed to investigate the apparent difference in the correlation between tear glucose and blood in these subpopulations.

The extremely low glucose concentrations in tear fluid, more than 100 times lower than in blood, raise questions about the physiologic role of tear glucose. Future studies are needed to address the correlation between tear and blood glucose in hypoglycemic and hyperglycemic states and in the presence of diabetes.

Grant funding/support: This research was supported by the National Institutes of Health Grant DK-55348 (to S.A.A.).

Financial Disclosures: S.A.A. is the scientific founder of Glucose Sensing Technologies LLC, a company developing glucose-sensing contact lenses.

Acknowledgments: We thank Drs. Gary Foulks and Cholapadi Sundar-Raj for helpful discussions and critical reviews of the manuscript.

References

1. Daum KM, Hill RM. Human tear glucose. *Invest Ophthalmol Vis Sci* 1982; 22:509–14.
2. LeBlanc JM, Haas CE, Vicente G, Colon LA. Evaluation of lacrimal fluid as an alternative for monitoring glucose in critically ill patients. *Intensive Care Med* 2005;31:1442–5.

3. Jin Z, Chen R, Colon LA. Determination of glucose in submicroliter samples by CE-LIF using precolumn or on-column enzymatic reactions. *Anal Chem* 1997;69:1326–31.
4. Chatterjee PR, De S, Datta H, Chatterjee S, Biswas MC, Sarkar K, et al. Estimation of tear glucose level and its role as a prompt indicator of blood sugar level. *J Indian Med Assoc* 2003;101:481–3.
5. Sen DK, Sarin GS. Tear glucose levels in normal people and diabetic patients. *Br J Ophthalmol* 1980;64:693–5.
6. Gasset AR, Braverman LE, Fleming MC, Arky RA, Alter BR. Tear glucose detection of hyperglycemia. *Am J Ophthalmol* 1968;65:414–20.
7. Lane JD, Krumholz DM, Sack RA, Morris C. Tear glucose dynamics in diabetes mellitus. *Curr Eye Res* 2006;31:895–901.
8. Vanhaeringen NJ, Glasius E. Collection method dependent concentrations of some metabolites in human tear fluid, with special reference to glucose in hyperglycemic conditions. *Albrecht Von Graefes Arch Klin Exp Ophthalmol* 1977;202:1–7.
9. Taormina CR, Baca JT, Finegold DN, Asher SA, Grabowski JJ. Analysis of tear glucose concentration with electrospray ionization mass spectrometry. *J Am Soc Mass Spectrom* 2007;18:332–6.
10. Alexeev V, Das S, Finegold D, Asher S. Photonic crystal glucose-sensing material for noninvasive monitoring of glucose in tear fluid. *Clin Chem* 2004;50:2353–60.
11. Badugu R, Lakowicz J, Geddes C. A glucose sensing contact lens: a non-invasive technique for continuous physiological glucose monitoring. *J Fluoresc* 2003;13:371–4.
12. March WF, Mueller A, Herbrechtsmeier P. Clinical trial of a noninvasive contact lens glucose sensor. *Diabetes Technol Ther* 2004;6:782–9.
13. March WF, Smith FE, Herbrechtsmeier P, Domschke A, Morris C. Clinical trial of a non-invasive ocular glucose sensor. *Diabetes 61st Scientific Sessions of the American Diabetes Association*, June 22–26, 2001, Philadelphia. *Amer Diabetes Assoc* 2001;50:A125.
14. Chen R, Jin Z, Colon LA. Analysis of tear fluid by CE/LIF: a noninvasive approach for glucose monitoring. *J Capillary Electrophor* 1996;3:243–8.
15. Kilp H, Heisig B. Glucose and lactate concentration in tears of rabbits following mechanical stress and wearing of contact lenses. *Albrecht Von Graefes Arch Klin Exp Ophthalmol* 1975;193:259–67.
16. Domschke A, March WF, Kabilan S, Lowe C. Initial clinical testing of a holographic non-invasive contact lens glucose sensor. *Diabetes Technol Ther* 2006;8:89–93.
17. Badugu R, Lakowicz J, Geddes C. A glucose-sensing contact lens: from bench top to patient. *Curr Opin Biotech* 2005;16:100–7.

Previously published online at DOI: 10.1373/clinchem.2006.078543

Microtransponder-Based Multiplex Assay for Genotyping Cystic Fibrosis, Xin Lin,¹ James A. Flint,¹ Marco Azaro,¹ Thomas Coradetti,¹ Wesley M. Kopacka,¹ Deanna L. Streck,² Zhuoying Wang,¹ James Dermody,² and Wlodek Mandeck^{1*} (¹PharmaSeq, Inc., Monmouth Junction, NJ; ²Department of Microbiology & Molecular Genetics, University of Medicine and Dentistry, New Jersey-New Jersey Medical School, Newark, NJ; *address correspondence to this author at: PharmaSeq, Inc., 11 Deer Park Drive, Suite 104, Monmouth Junction, NJ 08852; fax 732-355-0102, e-mail mandeck@pharmaseq.com)

Background: We developed and evaluated a genotyping assay for detection of 50 cystic fibrosis (CF) mutations. The assay is based on small (500 μm) electronic chips, radio frequency (RF) microtransponders (MTPs). The chips are analyzed on a unique fluorescence and RF readout instrument.

Methods: We divided the CF assay into 4 panels: core, Hispanic, African-American, and Caucasian. We amplified 18 CF transmembrane regulator (CFTR) DNA frag-

ments covering 50 mutations by use of multiplex PCR using 18 *CFTR* gene-specific primer pairs. PCR was followed by multiplex allele-specific primer extension (ASPE) reactions and hybridization to capture probes synthesized on MTPs. We used 100 ASPE primers and 100 capture probes. We performed fluorescence measurements of hybridized MTP kits and assay analysis using a custom automated bench-top flow instrument.

Results: We validated the system by performing the assay on 23 commercial DNA samples in an internal study and 32 DNA samples in an external study. For internal and external studies, correct calls were 98.8% and 95.7%, false-positive calls 1.1% and 3.9%, and false-negative calls 0.12% and 0.36%, respectively.

Conclusions: The MTP-based multiplex assay and analysis platform can be used for CF genotyping.

© 2007 American Association for Clinical Chemistry

Cystic fibrosis (CF) is caused by one or more mutations in the gene encoding for the CF transmembrane conductance regulator (CFTR) protein. CF occurs when both copies of the *CFTR* gene function abnormally, and one functional copy is sufficient to prevent the disease. In the Caucasian population, CF is inherited with a frequency of 1:3300, making it the most lethal inherited disease of childhood, but carrier frequency and incidence of CF vary with race and ethnic group (1). A single mutation causing loss of the phenylalanine residue at position 508 ($\Delta F508$) accounts for nearly 70% of all mutations observed in Caucasians with CF, but more than 1000 other mutations of the *CFTR* gene have been reported in all races and ethnic groups. In May 2001, the American College of Medical Genetics published a recommended panel of 25 mutations and 6 polymorphisms for population-based CF screening (2).

We describe a new platform for performing a multiplexed genotyping assay based on radio frequency (RF) microtransponders (MTPs) and provide a working example, the CF assay. CF mutations tested and the rationale are provided in Table 1 and Supplemental Data (see the Data Supplement that accompanies the online version of this article at <http://www.clinchem.org/content/vol53/issue7>). We designed this assay to be ethnic-group specific, thus simplifying the design and potentially reducing costs. The mutations are grouped into 4 panels: core, Caucasian, Hispanic, and African-American. Because the assay is ethnic specific, efficiency is increased, with fewer DNA probes and reagents needed. A patient would be tested with 2 panels, the core panel and one ethnic panel; more than one ethnic panel might be used for patients with complex ethnic backgrounds.

The key element of the assay method is the MTP (Fig. 1A), a monolithic $500\ \mu\text{m} \times 500\ \mu\text{m}$ integrated circuit chip that can transmit its identification code by RF. Each chip consists of photocells, read-only memory (ROM), transmit

logic circuitry, and an antenna loop. Visible light, typically red or green, is pulsed at 1.5 MHz to provide power and a stable clocking signal for the logic circuitry. The circuitry accesses the contents of ROM (the ID value) and modulates the current through the antenna in correspondence with the ID value. The resulting variable magnetic field in the vicinity of the MTP can then be measured with a nearby receiving coil and decoded to provide the ID value, which identifies the oligonucleotide immobilized on the MTP. The current MTP design uses 10 bits to encode the ID value, allowing 1024 unique values; however, the ROM contains an additional 40 unused bits, so the MTPs could be manufactured to have as many as 2^{50} ($\sim 10^{15}$) unique ID values. Before use, the MTPs are coated with a polymer that places both hydroxy and amino groups on the surface of the chip. Such derivatized MTPs are subjected to oligonucleotide synthesis.

In preparation for the flow reader analysis, the MTPs are suspended in a liquid medium that prevents sedimentation of MTPs but allows flow characteristics comparable to water when sheared. The suspension is repeatedly passed through a narrow channel of the instrument, where the ID values are read and fluorescence measurements are made. The flow system is designed to support a transfer rate of up to 1000 MTPs/s. The time needed to read the ID can be as short as 300 μs and the time to read fluorescence 1–2 ms. Multiple forward and reverse passes, typically 50 total passes, of the MTPs through the flow channel are required to obtain enough data for analysis. The instrument in the present study, Tsunami IV, uses a 532-nm, 300-mW laser for both RF identification and fluorescence at a single location on one side of the flow channel. We used custom software named Retro for data analysis. Both the flow reader and MTPs are described in more detail in a recent report (3).

The principle for detecting mutations is allele-specific primer extension (ASPE) (4, 5) on the PCR-amplified *CFTR* DNA; the schematic of the assay is shown in Fig. 1B. For each mutation, 2 primers were prepared, one specific to the wild-type allele and another specific to the mutant allele. The sequence differences between the 2 primers are the tag sequence at the 5' end and a single nucleotide at the 3' end (an "anchor" sequence). Thus, for any particular allele, only 1 primer was extended in a reaction with DNA polymerase in the presence of 4 dNTPs. After the ASPE reaction, the target DNA was hybridized to a capture probe, the sequences of which are complementary to tag sequences commonly referred to as universal tags (4, 6–8). The capture probe is a synthetic oligonucleotide (24 nucleotides) covalently bound to the MTP surface. Because the tag sequence was present at the 5' end of allele-specific primers, the capture reaction was very specific. In the ASPE reaction, we used biotin-labeled dCTP in place of dCTP. Thus, the ASPE target typically contained several biotin moieties, which were subse-

Table 1. CF genotyping results for the core panel from internal validation.^a

Sample	Allelic Variant	1	2	3	4	5	6	7	8	9	10	11
		G542X	A455E	G551D	3659delC	R334W	1078delT	1717-1G>A	R553X	R560T	R1162X	R347P
1	Wild-type DNA
2	ΔF508/ΔF508
3	3120 + 1G>A/621 + 1G>T
4	R553/ΔF508	m	.	.	.
5	G551D/wild-type	.	.	m
6	3659delC/ΔF508	.	.	.	m
7	ΔI507/wild-type
8	711 + 1G>T/621 + 1G>T
9	621 + 1G>T/ΔF508	M*	.	.	.
10	G85E/621 + 1G>T
11	A455E/ΔF508	.	m
12	R560T/ΔF508	m	.	.
13	N1303K/G1349D
14	G542X/G542X	M
15	W1282X/wild-type
16	2789 + 5G>A/2789 + 5G>A
17	3849 + 10C>T/3849 + 10C>T
18	1717-1G>T/wild-type	m
19	R1162X/wild-type	m	.
20	R347P/G551D	.	.	m	m
21	R334W?	m
22	R117H/ΔF508
23	2184delA/ΔF508
24	1898 + 1G>A/ΔF508

^a Mutation calls for 2 alleles are abbreviated as follows: dot, wild-type/wild-type; m, wild-type/mutant; M, mutant/mutant; *, incorrect call; blank, not assayed for the particular mutation in accordance with the work plan. Mutation panels are defined as follows: core, 1–24 (using the numbers on the top of table); Caucasian, M1101K, Y1092X, 2183delAA>G, 3199del6*, 394delTT, 405 + 3A>C; Hispanic, ΔF311, D1270N, G330X, I506T, R75X, S549N, W1089X, Y1092X, 1812-1G>A, 2055del9>A, 2183delAA>G, 3199del6*, 406-1G>A, 935delA; African-American, ΔF311, A559T, G480C, R1066C, R1158X, S1255X, S549N, 1812-1G>A, 2307insA, 405 + 3A>C, 444delA, 3791delC. Mutation panels are based on literature data (14–19). Genotyping results for Caucasian, Hispanic, and African-American panels are presented in the online Data Supplement.

The treated multiplex PCR products (10–20 ng of each DNA fragment) were added to the ASPE reaction mixture, final volume 40 μL, containing 20 mmol/L Tris-HCl (pH 8.0), 50 mmol/L KCl, 25 mmol/L allele-specific primers, 5 μmol/L biotin-CTP, 0.1% Triton-100, 28 μmol/L dCTP, 100 μmol/L dNTP (dCTP⁻), and 3 units Tsp DNA polymerase. The reactions were incubated at 96 °C for 2 min to denature DNA, followed by 30 PCR cycles (94 °C for 30 s, 60 °C for 1 min, and 74 °C for 2 min) and 72 °C for 7 min.

Hybridization of MTPs was performed in the 1× prehybridization buffer [50 mmol/L Tris-HCl, pH 8.0, 150 mmol/L sodium chloride, 0.1% (wt/vol) SDS, 0.5% (wt/vol) Ficoll (type 400), 5 mmol/L EDTA, pH 8.0, 200 μg/mL sheared, denatured salmon sperm DNA, 1 μg/μL BSA] at 48 °C for 10 min. After removing the prehybridization buffer, the MTPs were hybridized in 1× hybridization solution (80 μL ASPE products and 80 μL 2× hybridization buffer) at 48 °C for 2 h and rinsed 3 times.

Streptavidin-phycoerythrin conjugate was diluted 1:10 in PBS (1.06 mmol/L potassium phosphate monobasic, 155.17 mmol/L sodium chloride, 2.97 mmol/L sodium phosphate dibasic, pH 7.4), and 10 μL was added to 120 μL 1× washing buffer at a final concentration of 8 μg/mL. The MTPs bearing the hybridized DNA were incubated in the above solution for 30 min at room temperature in the dark, rinsed, and analyzed.

quently visualized as a result of a binding reaction with phycoerythrin-labeled streptavidin (phycoerythrin is a pigment-carrying, highly fluorescent protein from red algae). The fluorescence was then read in the flow reader instrument.

Eighteen pairs of PCR primers were designed using an in-house custom software package, SimuPlex (9). SimuPlex accepts a sequence file comprising all the loci for which PCR primers are to be designed. The SimuPlex then identifies all qualified primers that meet the criteria defined in the parameter file and executes a local BLAST (Basic Local Alignment Search Tool) search that filters out undesired primers. Once the candidates are filtered, SimuPlex creates a “seed” multiplex set and then uses a simulated annealing algorithm to search the surrounding solution space for even better multiplex sets. The melting temperature (T_m) and free-energy calculations are based

on the most accurate and up-to-date formulas and thermodynamic data sets (10, 11). The results of a multiplex PCR reaction for which primers were designed using SimuPlex software is shown in Fig. 1C.

Allele-specific primers containing 24-nt tag sequences were designed using 3 custom programs written in Python: ExtractProbes.py, FindOptProbe.py, and Tags2Probes.py. The tag sequences were at the 5' end of the primers, and allele-specific sequences were at the 3' end. The allele-specific sequences varied in length, but always possessed a T_m of 50 °C. For each biallelic single nucleotide polymorphism analyzed by ASPE, 2 allele-specific primers (ASP) were synthesized, with each ASP differing in the tag sequence and in the polymorphic nucleotide contained at its 3' terminus.

We conducted 2 separate series of experiments to validate the performance of the assay. In the internal

Table 1. Continued

12	13	14	15	16	17	18	19	20	21	22	23	24
2789 + 5G>A	G85E	N1303K	R117H	W1282X	2184delA	3120 + 1G>A	621 + 1G>T	ΔF508	Δ1507	1898 + 1G>A	3849 + 10kbC>T	711 + 1G>T
.
.	M
.	m	m
.	m
.
.	m
.	.	m*	M*	.	.	.	m	.	m	.	.	m
.	m	m
.	m	.	.	.	m*	.	m
.	m
.	.	m	m
.	.	m*	m*	m*	.	.	.
.
M
.	M	.
.
.
.
.
.	.	.	m	m
.	m
.	m	.	m	.	.

study, we used 23 standard (Coriell) genomic DNA samples. In addition, we used 32 coded genomic DNA samples in an external study completed in Dr. Dermody’s laboratory at the University of Medicine and Dentistry of New Jersey. During the course of this project, >100 CF reagent sets were prepared. Each reagent set consisted of a vial containing derivatized MTPs that compose the mutation panel and the assay file on electronic media. Typically, 3 MTPs were used for each probe to achieve multiple readouts for statistical accuracy.

The results from the internal study (Table 1) indicate that correct calls were 98.8% of all determinations (807 total calls), and false-positive and false-negative calls were 1.1% and 0.12%, respectively. The results from the external study are shown in the Supplemental Data. Correct calls were 95.7% of all determinations (1086 total calls), and false-positive and false-negative calls were 3.9% and 0.36%, respectively. In addition, 27 synthetic 60-nt oligonucleotides were designed to simulate DNA mutations not present in the Coriell DNA samples. Assays performed on the synthetic samples resulted in 100% correct calls of homozygous mutation.

We are generally pleased with the results obtained in both the internal and external testing. The overall percentage of correct calls was high: 98.8% and 95.6%, respectively. Especially encouraging were high fluorescence ratios (wild type-to-mutant oligo probe), approaching 100 in many cases, indicating a high potential of the assay for DNA testing, and in particular CF testing. The wrong calls seem to be clustered for specific mutations, suggesting difficulties with certain oligonucleotides or PCR products.

In summary, MTPs were used as solid phase in a CF assay. Although the reported rate of false positives (1%–4%) is higher than in commercially available CF assays [Luminex (12), Roche, and Applera (13)], we are confident that it can be improved, because the biochemical basis of the assay is well understood and the biochemical principle is similar to that implemented in the Luminex CF assay (12). The main advantage of the MTP platform is the large number of ID codes available, currently 1024 but readily expandable. The expansion might be justified if the number of mutations being tested for increases, or if other types of assays require a higher multiplex level.

Grant funding/support: This work was funded by National Institutes of Health Grant HL074607.

Financial disclosures: The authors associated with PharmaSeq, Inc., have equity interest in the company. J.D. is a consultant to the company.

Acknowledgments: We thank Richard G. Morris and Marvin Schwalb for helpful discussions and encouragement.

References

1. Palomaki GE, FitzSimmons SC, Haddow JE. Clinical sensitivity of prenatal screening for cystic fibrosis via CFTR carrier testing in a United States panethnic population. *Genet Med* 2004;6:405–14.
2. American College of Obstetrics and American College of Medical Genetics. Preconception and prenatal carrier screening for cystic fibrosis: clinical and laboratory guidelines. Washington, DC: American College of Obstetrics and Gynecology, 2001:32pp.
3. Mandecki W, Ardelt B, Coradetti T, Davidowitz H, Flint J, Huang Z, et al. Microtransponders, the miniature RFID electronic chips, as platforms for cell growth in cytotoxicity assays. *Cytometry A* 2006;69:1097–105.
4. Ye F, Li MS, Taylor JD, Nguyen Q, Colton HM, Casey WM, et al. Fluorescent microsphere-based readout technology for multiplexed human single nucle-

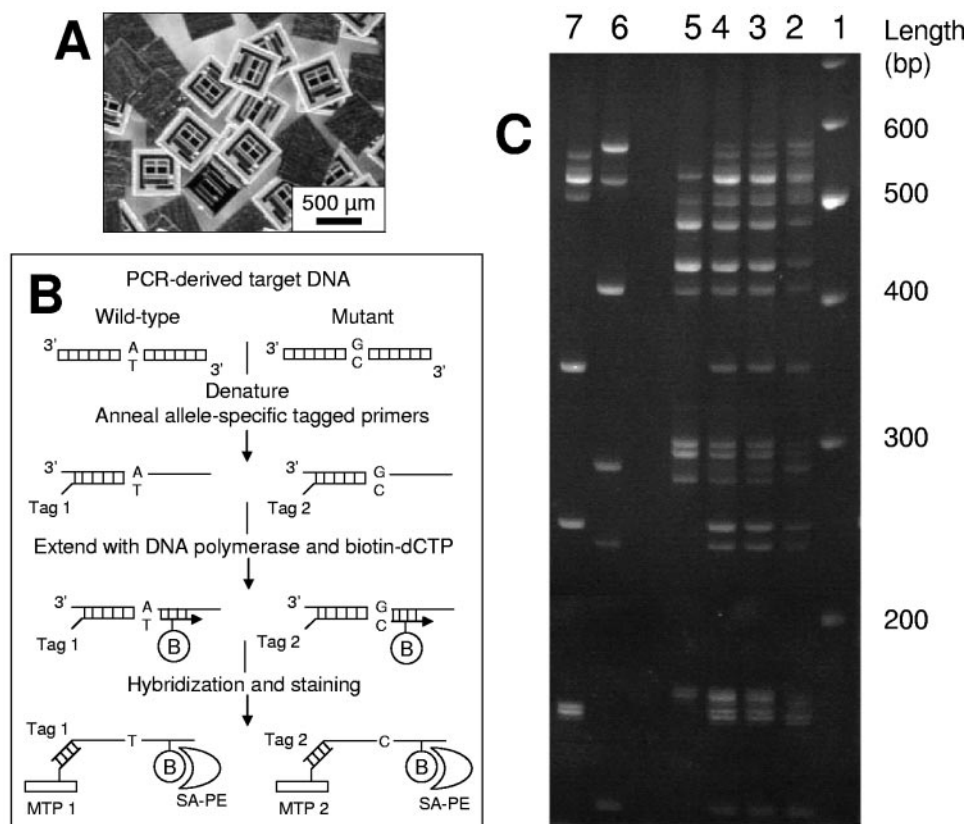


Fig. 1. (A), microtransponders used in the assay, the integrated circuit side and the back of the microtransponder (*dark gray squares*).

To coat MTPs, the chips were treated with coating solution containing 3-aminopropyltriethoxysilane. Capture probes were synthesized on the coated MTPs at PrimeSyn. The capture probe sequences were complementary to the tag sequences in each allele-specific primer; in addition, they had a spacer of 9 T residues at the 3' end. (B), schematic of the assay. (C), multiplex PCR results. Eighteen DNA fragments were PCR amplified from the CFTR gene. Lane 1, 100 bp DNA ladder; lane 2, 18-plex standard; lane 3, 18-plex-PCR-1; lane 4, 18-plex-PCR-2; lane 5, 6-plex-PCR-1; lane 6, 6-plex-PCR-2; lane 7, 6-plex-PCR-3. The presence of proper PCR products was confirmed on a 10% polyacrylamide Tris-boric acid-EDTA gel. All 18 DNA fragments can be readily identified by PAGE (lanes 5–7) when the PCR is done in 3 sets of 6 amplicons each.

To construct the multiplex primer set, all the primer pairs were combined at a final concentration of 74 nmol/L each, although in some cases an adjustment was made to achieve more efficient amplification. PCR reactions were performed on the GenAmp PCR System 9700 (Applied Biosystems). The 18- and 6-plex amplifications were performed in 30- μ L reactions containing 3 units AmpliTaq Gold DNA polymerase (Applied Biosystems), 10 mmol/L Tris-HCl (pH 8.3), 50 mmol/L KCl, 1.5 mmol/L MgCl₂, 250 μ mol/L deoxynucleotide triphosphates (dNTPs: dATP, dCTP, dGTP, and dTTP), 6 μ L primer mix, and 0.65 μ L DNA template at a concentration of ~184.4 ng/ μ L. Forty thermal cycles were implemented, and the extension temperature was between 55 and 64 °C.

Equal volumes of all PCR products to be simultaneously assayed were pooled and enzymatically treated to degrade the excess PCR primers and dNTPs using 1 unit shrimp alkaline phosphatase and 2 units Exol exonuclease per 10 μ L of the PCR products in a reaction performed at 37 °C for 30 min, followed by a 15-min incubation at 80 °C to inactivate the enzymes.

- otide polymorphism analysis and bacterial identification. *Hum Mutat* 2001; 17:305–16.
- Taylor JD, Briley D, Nguyen Q, Long K, Lannone MA, Li MS, et al. Flow cytometric platform for high-throughput single nucleotide polymorphism analysis. *BioTechniques* 2001;30:661–9.
 - Tm Bioscience. <http://www.tmbioscience.com/tm100universalarray.php> (accessed February 2007).
 - Wang DG, Fan JB, Siao CJ, Berno A, Young P, Sapolsky R, et al. Large-scale identification, mapping and genotyping of single nucleotide polymorphisms in the human genome. *Science* 1998;280:1077–82.
 - Gerry NP, Witowski NE, Day J, Hammer RP, Barany G, Barany F. Universal DNA microarray method for multiplex detection of low abundance point mutations. *J Mol Biol* 1999;292:251–62.
 - Azaro MA, Lin X, Mandecki W. SimuPlex: primer design software for multiplex PCR. Poster presentation, NIH Small Business Innovation Research Conference, July 2005, Bethesda, MD.
 - SantaLucia JJ, Hicks D. The thermodynamics of DNA structural motifs. *Annu Rev Biophys Biomol Struct* 2004;33:415–40.
 - The Santa Lucia Lab. <http://ozone3.chem.wayne.edu> (accessed February 2007).
 - Strom CM, Janeczko R, Quan F, Wang SB, Buller A, McGinniss M, et al. Technical validation of Tm Biosciences Luminex-based multiplex assay for detecting the American College of Medical Genetics recommended cystic fibrosis mutation panel. *J Mol Diagn* 2006;8:371–5.
 - Strom CM, Clark DD, Hantash FM, Rea L, Anderson B, Maul D, et al. Direct visualization of cystic fibrosis transmembrane regulator mutations in the clinical laboratory setting. *Clin Chem* 2004;50:836–45.
 - CDC web site: http://www.cdc.gov/genomics/gtesting/ACCE/FBR/CF/CFClVal_19c.htm (accessed February 2007).
 - Palomaki GE, Haddow JE, Bradley LA, FitzSimmons SC. Updated assessment of cystic fibrosis mutation frequencies in non-Hispanic Caucasians. *Genet Med* 2002;4:90–4.
 - Kazazian HH. Population variation of common cystic fibrosis mutations. *Hum Mutat* 1994;4:167–77.
 - Tomaiuolo R, Spina M, Castaldo G. Molecular diagnosis of cystic fibrosis: comparison of four analytical procedures. *Clin Chem Lab Med* 2003;41:26–32.
 - Heim RA, Sugarman EA, Allitto BA. Improved detection of cystic fibrosis mutations in the heterogeneous U.S. population using an expanded, pan-ethnic mutation panel. *Genet Med* 2001;3:168–76.
 - Bobadilla JL, Macek M Jr, Fine JP, Farrell PM. Cystic fibrosis: a worldwide analysis of CFTR mutations: correlation with incidence data and application to screening. *Hum Mutat* 2002;19:575–606.

Optimization of High-Resolution Melting Analysis for Low-Cost and Rapid Screening of Allelic Variants of *Bacillus anthracis* by Multiple-Locus Variable-Number Tandem Repeat Analysis,

Daniela Fortini,¹ Andrea Ciaramarconi,² Riccardo De Santis,² Antonio Fasanella,³ Antonio Battisti,⁴ Raffaele D'Amelio,^{5,6} Florigio Lista,² Antonio Cassone,¹ and Alessandra Carattoli^{1*} (¹ Department of Infectious, Parasitic and Immune-Mediated Diseases, Istituto Superiore di Sanità, Rome, Italy; ² Molecular Biology Section, Army Medical and Veterinary Research Center, Rome, Italy; ³ Istituto Zooprofilattico Sperimentale della Puglia e della Basilicata-Anthrax Reference Institute of Italy, Foggia, Italy; ⁴ Istituto Zooprofilattico Sperimentale delle Regioni Lazio e Toscana, Rome, Italy; ⁵ Cattedra di Allergologia e Immunologia Clinica, II Facoltà di Medicina, Università di Roma "La Sapienza", Rome, Italy; ⁶ Direzione Generale della Sanità Militare, Rome, Italy; * address correspondence to this author at: Department Infectious, Parasitic and Immuno-Mediated Diseases, Istituto Superiore di Sanità, Viale Regina Elena 299, 00161 Rome, Italy; fax 39-06-49387112, e-mail alecara@iss.it)

Background: Molecular genotyping of *Bacillus anthracis*, the etiologic agent of anthrax, is important for differentiating and identifying strains from different geographic areas and for tracing strains deliberately released in a bioterrorism attack. We previously described a multiple-locus variable-number tandem repeat (VNTR) analysis (MLVA) based on 25 marker loci. Although the method has great differentiating power and reproducibility, faster genotyping at low cost may be requested to accurately identify *B. anthracis* strains in the field.

Methods: We used the High Resolution Melter-1 (Idaho Technology) and a saturating dye of double-stranded DNA (LCGreen I) to identify alleles via PCR and melting-curve analysis of the amplicons. We applied high-resolution melting analysis (HRMA) to a collection of 19 *B. anthracis* strains.

Results: HRMA produced reproducible results for 6 of the 25 *B. anthracis* loci tested. These easily interpretable and distinguishable melting curve results were consistent with MLVA results obtained for the same alleles. The feasibility of this method was demonstrated in testing of different allelic variants for the 6 selected loci.

Conclusions: The described HRMA application for screening *B. anthracis* VNTR loci is fast and widely accessible and may prove particularly useful under field conditions.

© 2007 American Association for Clinical Chemistry

Bacillus anthracis, the etiologic agent of anthrax, is a spore-forming gram-positive bacterial species that, because of its highly pathogenic nature, environmental resistance, and relatively easy dissemination, is included among the major pathogens considered likely bioterrorism agents. Although genetically homogeneous (1), this

bacterium has been genotyped (2), and molecular genotyping of *B. anthracis* played an important role in differentiating and identifying the strains used in the 2001 bioterrorism attack in the US (1,2). Recent efforts to evaluate the diversity of *B. anthracis* isolates from different geographic areas have improved our knowledge of the phylogeny and geographic distribution of different genetic variants (gene clusters) of this species (3–7). Studies have also tried to trace strains deliberately released into the environment back to their origins (8). The method universally adopted for genotyping *B. anthracis* strains is multiple-locus variable-number tandem repeat (VNTR) analysis (MLVA). This technique involves amplifying multiple chromosomal loci carrying VNTRs and sizing the fragments to classify allelic variants on the basis of length polymorphisms (8,9). The level of intraspecific polymorphism for tandemly repeated sequences varies among loci, and this variation needs to be evaluated experimentally with collections of representative strains.

Previous reports proposed that the MLVA method be used with 6 chromosomal and 2 plasmid marker loci (MLVA8) and that amplicon size be analyzed by agarose gel electrophoresis (9–11). This method has recently been updated for the analysis of 25 marker loci (MLVA25) by measuring PCR fragment size with an automated capillary DNA sequencer (12). The latter method allows a more sensitive differentiation of closely related strains, but accurate analyses require expensive platforms and well-organized laboratory facilities. In this study, we have examined the feasibility of a high-resolution melting analysis (HRMA) for rapidly and easily recognizing and differentiating VNTR allelic variants. This technique uses the High Resolution Melter-1 (HR-1; Idaho Technology), which has recently been adopted for genotyping and screening mutations in several different research and clinical applications (13–17). This method consists of a rapid (2 min after the PCR), closed-tube assay that detects sequence variation within specific genetic loci via melting curve analysis of the amplicons with a saturating dye of double-stranded DNA (LCGreen I). We applied HRMA initially to a *B. anthracis* collection at the Istituto Superiore di Sanità, Rome, Italy. This collection consists of 12 strains—10 previously analyzed with MLVA25 and 2 new isolates of a *B. anthracis* strain involved in a recent case of human anthrax in Italy (18). One of these latter isolates was from necropsy materials from a sheep killed by anthrax, and one was isolated from the shepherd's cutaneous lesion. Eight of the 10 previously characterized strains were from animals (ST1761 and ST2844 strains belong to *B. anthracis* clusters B2 and D, respectively), and 2 were vaccine strains (Pasteur and Sterne strains) (Table 1). We extracted total genomic DNA from the 12 strains and amplified the 25 VNTR loci as previously described (12) with the LCGreen I dye to fluorescently label double-stranded DNA in a LightCycler 2.0 instrument (Roche Diagnostics).

Our study showed that DNA quality and final concentration were critical variables for obtaining reproducible melting curves for identical loci. We tested the reproduc-

Table 1. Allelic variants for 6 selected loci for the *Bacillus anthracis* *B. anthracis* strains analyzed in this study.^a

Strain or genotype ^c	Source	VrrA	VrrB1	VrrB2	BamS1	BamS23	BamS31	Cluster ^b
LT1	Animal	10	16	7	13	11	65	A1a
LT2	Animal	10	16	7	13	11	64	A1a
LT3	Animal	10	16	7	13	11	65	A1a
LT4	Animal	10	16	7	13	11	64	A1a
LT5	Animal	10	16	7	13	11	64	A1a
Pasteur	Vaccine	10	16	7	13	11	64	A1a
Sterne	Vaccine	10	16	7	16	11	65	A3a
Ferrara	Animal	10	16	6	13	11	64	A1a
ST1761	Animal	9	15	7	14	10	84	B2
ST2844	Animal	11	16	8	11	10.5	15	D
Sheep	Animal	9	11	7	14	10	83	B3
Farmer	Human	9	11	7	14	10	83	B3
12 ^c	Animal	10	16	7	13	5	64	A1a
31 ^c	Animal	10	16	7	13	11	55	A1a
35 ^c	Animal	8	16	7	13	11	64	A1a
42 ^c	Animal	10	12	7	13	11	64	A3a
44 ^c	Animal	10	16	7	13	9	64	A3a
55 ^c	Animal	11	16	4	11	10.5	15	D
61 ^c	Animal	9	19	7	11	10	64	B1

^a Allelic variants are reported as the number of repeat units as measured by the MLVA25 method in Lista et al. (12).

^b *B. anthracis* clusters were previously assigned in the MLVA25 genotype analysis [Lista et al. (12)].

^c Selected reference strains of definite genotypes were included to analyze all the known allelic variants that have been described for the 6 loci. Numbers refer to genotypes of strains reported in the supplementary data file in Lista et al. (12).

ibility of this assay with triplicate samples of 0.5–500 ng of column-purified chromosomal DNA and PCR products as potential templates for PCR and HRMA. We also tested DNA obtained by boiling bacterial suspensions for 20 min (19); we compared the results with these DNA templates with those obtained for column-purified chromosomal DNA. We obtained optimal reproducibility with 20–40 ng of column-purified chromosomal DNA per PCR reaction tube and further improved reproducibility by reducing the amount of LCGreen I dye used per reaction tube to half that recommended by the manufacturer (13–17). Reducing the dye amount probably limits the availability of the fluorescent dye, thereby producing a constant number of labeled molecules; use of half the recommended LCGreen I produces lower fluorescent signals in the PCR (see Fig. 1A in the Data Supplement that accompanies the online version of this Technical Brief at <http://www.clinchem.org/content/vol53/issue7>). This modification produces better melting curve reproducibility in the HRMA for different amplicons and different amounts of DNA templates in each PCR reaction tube [see (16) and Figs. 1 and 2 in the online Data Supplement].

Under these conditions, HRMA gave reproducible intraexperimental melting curves for the same alleles, which permitted the differentiation of alleles with different numbers of repeat units (ru) (Fig. 1). Bovo et al. (20) have described multiple-band artifacts that are produced by improper reannealing of repetitive microsatellite sequences when too many PCR cycles are used. We did not observe this effect for the *B. anthracis* loci under our experimental conditions (see above and Fig. 3 in the online Data Supplement). These observations suggest that

HRMA can be used as an initial and low-cost method for screening *B. anthracis* VNTR allelic variants. We also tested the interexperimental reproducibility of HRMA by comparing the melting curves obtained for the same allelic variant in different experimental runs. Despite our application of the standardized conditions we have described, interexperimental reproducibility needs to be improved. Melting curve shape was reproducible, but the curves did not always perfectly overlap. Nonetheless, our use of triplicate measurements of each reference allelic variant can improve interexperimental comparisons of allele melting curves.

We applied this experimental approach to all 25 *B. anthracis* VNTR loci and eventually selected 6 loci that yielded easily differentiated melting curves and a high capacity for distinguishing different strains.

We then included 7 additional strains (12) with different allelic variants for these 6 loci in the collection of tested strains (Table 1) to verify the feasibility of HRMA to detect all the different variants previously described for these loci (Fig. 1).

For the large amplicon of the BamS31 locus, which MLVA25 scored as having a high differentiating power, we added a 5'-CGC CGC CCG CCG CCC GCC-3' clamp at the 5' ends of the previously described forward and reverse primers to improve melting curve resolution for alleles carrying 15, 55, 64, 65, 83, or 84 ru (panel BamS31 in Fig. 1) (12, 17). It is noteworthy that HRMA was able to correctly identify all of the other allelic variants (differing by just 1 ru to 69 ru) for the rest of the loci, with the exception of the BamS23 10.5 ru variant, which we could not differentiate from the 10 ru allele. For example, the

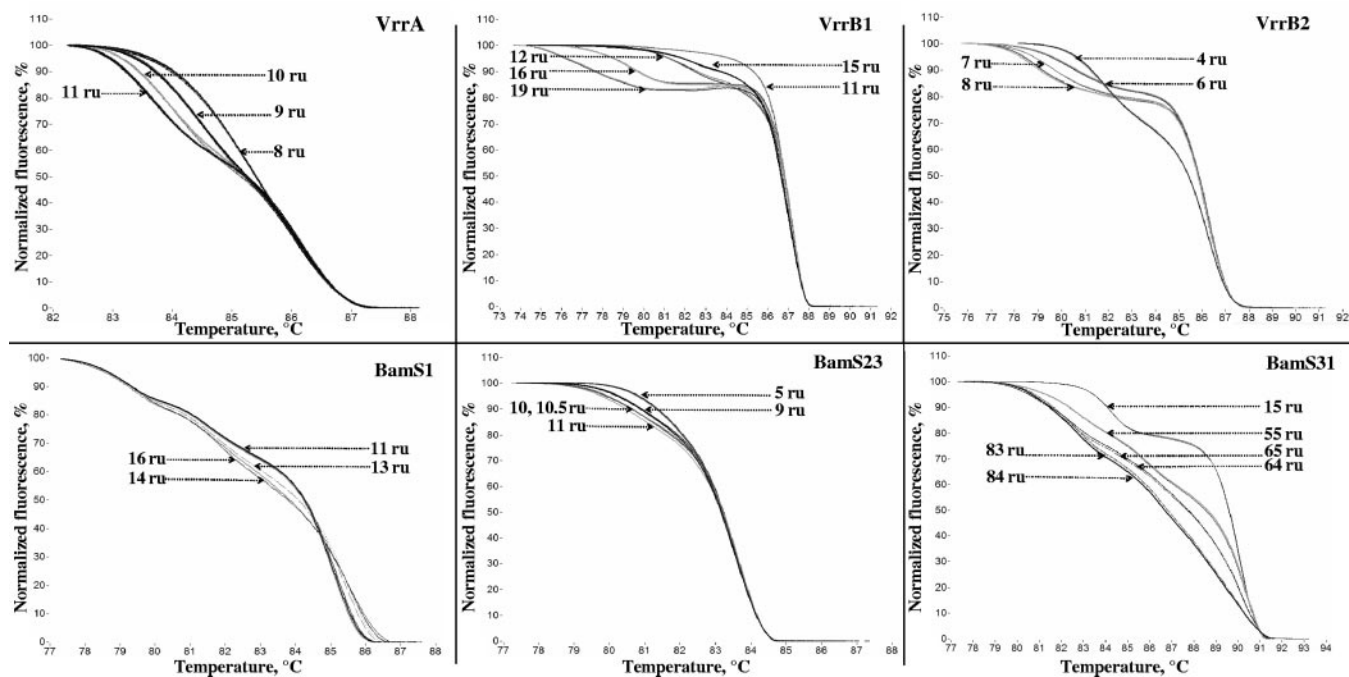


Fig. 1. Representative high-resolution melting curves in duplicate for 6 VNTR loci.

Half of the amount of LCGreen I fluorescent dye recommended by the manufacturer was used in a LightCycler 2.0 instrument with an initial denaturation step at 94 °C for 3 min, followed by 36 cycles of denaturation at 94 °C for 20 s, annealing at 60 °C for 30 s, and extension at 68 °C for 2 min. In the final cycle, we evaluated amplicon melting curves by first denaturing the sample from 45 °C to 95 °C at a rate of 0.1 °C/s. Capillary tubes were then moved from the LightCycler to the HR-1 platform, and high-resolution melting curves were obtained by heating the tubes at a rate of 0.3 °C/s during data acquisition at 80 °C–100 °C for marker VrrA and at 75 °C–100 °C for the other markers. We used HR-1 software to analyze melting curves. Arrows indicate the different allelic variants identified for each locus. The ru characteristic for each specific allele variant is derived from the MLVA25 assay (12) and is presented in the Fig. next to each arrow.

allelic variants for the VrrA, VrrB1, and VrrB2 loci that differed by 1 ru yielded nicely differentiated melting curves (panels VrrA, VrrB1, and VrrB2 in Fig. 1). The assay is also reproducible, because duplicate amplifications and HR-1 analyses produced identical curves for each allelic variant (Fig. 1).

We applied optimized HRMA to a cluster analysis of the 12 strains. A genotype cluster analysis of the 6 loci evaluated with HRMA distinguished 7 genotypes, whereas a cluster analysis based on the MLVA results distinguished 10 genotypes (see Fig. 4 in the online Data Supplement). The HRMA method was still able to identify the major branches, however. HRMA was unable to separate the very close relationships between the LT5, LT2, LT4, and Pasteur strains (0.1 linkage distance) identified with the MLVA25 method (12).

We obtained identical allelic variants for the sheep and shepherd (farmer) isolates, demonstrating that the patient's cutaneous lesion was caused by the *B. anthracis* strain in the animal. This conclusion was tentatively suggested during the epidemiologic investigation of this anthrax case (18), and we have confirmed that inference. Based on the HRMA and the MLVA25 analyses, we have assigned these 2 strains to *B. anthracis* cluster B3.

Our application of the HRMA method to *B. anthracis* genotyping opens the possibility of a rapid screening method for *B. anthracis* VNTR loci and for implementing this diagnostic procedure in the field or in the first-event laboratory. HRMA may be helpful for evaluating *B.*

anthracis allelic variants if a large number of samples have to be rapidly analyzed and compared, as may be required in the event of a bioterrorism attack.

Grant/funding support: This work is supported by the Progetto Antrace- ISS-Ministero della Salute, within the framework of the "Italy-US Collaboration Program".

Financial Disclosures: None declared.

Acknowledgments: We are grateful to Claudia Lucarelli for her skillful assistance.

References

1. Read TD, Peterson SN, Tourasse N, Baillie LW, Paulsen IT, Nelson KE, et al. The genome sequence of *Bacillus anthracis* Ames and comparison to closely related bacteria. *Nature* 2003;423:81–6.
2. Hoffmaster AR, Fitzgerald CC, Ribot E, Mayer LW, Popovic T. Molecular subtyping of *Bacillus anthracis* and the 2001 bioterrorism-associated anthrax outbreak, United States. *Emerg Infect Dis* 2002;8:1111–6.
3. Fouet A, Smith KL, Keys C, Vaissaire J, Le Doujet C, Levy M, et al. Diversity among French *Bacillus anthracis* isolates. *J Clin Microbiol* 2002;40:4732–4.
4. Gierczynski R, Kaluzewski S, Rakin A, Jagielski M, Zasada A, Jakubczak A, et al. Intriguing diversity of *Bacillus anthracis* in eastern Poland: the molecular echoes of the past outbreaks. *FEMS Microbiol Lett* 2004;239:235–40.
5. Smith KL, DeVos V, Bryden H, Price LB, Hugh-Jones ME, Keim P. *Bacillus anthracis* diversity in Kruger National Park. *J Clin Microbiol* 2000;38:3780–4.
6. Merabishvili M, Natidze M, Rigvava S, Brusetti L, Raddadi N, Borin S, et al. Diversity of *Bacillus anthracis* strains in Georgia and of vaccine strains from the former Soviet Union. *Appl Environ Microbiol* 2006;72:5631–6.
7. Fasanella A, Van Ert M, Altamura SA, Garofolo G, Buonavoglia C, Leori G, et al. Molecular diversity of *Bacillus anthracis* in Italy. *J Clin Microbiol* 2005;43:3398–401.

8. Keim P, Van Ert MN, Pearson T, Vogler AJ, Huynh LY, Wagner DM. Anthrax molecular epidemiology and forensics: using the appropriate marker for different evolutionary scales [Review]. *Infect Genet Evol* 2004;4:205–13.
9. Jackson PJ, Walther EA, Kalif AS, Richmond KL, Adair DM, Hill KK, et al. Characterization of the variable-number tandem repeats in *vrA* from different *Bacillus anthracis* isolates. *Appl Environ Microbiol* 1997;63:1400–5.
10. Jackson PJ, Hill KK, Laker MT, Ticknor LO, Keim P. Genetic comparison of *Bacillus anthracis* and its close relatives using amplified fragment length polymorphism and polymerase chain reaction analysis. *J Appl Microbiol* 1999;87:263–9.
11. Keim P, Price LB, Klevytska AM, Smith KL, Schupp JM, Okinaka R, et al. Multiple-locus variable-number tandem repeat analysis reveals genetic relationships within *Bacillus anthracis*. *J Bacteriol* 2000;182:2928–36.
12. Lista F, Faggioni G, Valjevac S, Ciammaruconi A, Vaissaire J, le Doujet C, et al. Genotyping of *Bacillus anthracis* strains based on automated capillary 25-loci multiple locus variable-number tandem repeats analysis. *BMC Microbiol* 2006;6:33.
13. Margraf RL, Mao R, Highsmith WE, Holtegaard LM, Wittwer CT. Mutation scanning of the *RET* protooncogene using high-resolution melting analysis. *Clin Chem* 2006;52:138–41.
14. Graham R, Liew M, Meadows C, Lyon E, Wittwer CT. Distinguishing different DNA heterozygotes by high-resolution melting. *Clin Chem* 2005;51:1295–8.
15. Reed GH, Wittwer CT. Sensitivity and specificity of single-nucleotide polymorphism scanning by high-resolution melting analysis. *Clin Chem* 2004;50:1748–54.
16. Wittwer CT, Reed GH, Gundry CN, Vandersteen JG, Pryor RJ. High resolution genotyping by amplicon melting analysis using LCGreen. *Clin Chem* 2003;49:853–60.
17. Gundry CN, Vandersteen JG, Reed GH, Pryor RJ, Chen J, Wittwer CT. Amplicon melting analysis with labeled primers: a closed-tube method for differentiating homozygotes and heterozygotes. *Clin Chem* 2003;49:396–406.
18. Kreidl P, Stifter E, Richter A, Aschbacher R, Nienstedt F, Unterhuber H, et al. Anthrax in animals and a farmer in Alto Adige, Italy. *Euro Surveill* 2006;11:E060216.3.
19. Fasanella A, Losito S, Trotta T, Adone R, Massa S, Ciuchini F, et al. Detection of anthrax vaccine virulence factors by polymerase chain reaction. *Vaccine* 2001;19:4214–8.
20. Bovo D, Rugge M, Shiao Y-H. Origin of spurious multiple bands in the amplification of microsatellite sequences. *Mol Pathol* 1999;52:50–1.

Previously published online at DOI: 10.1373/clinchem.2007.085993

Quantification of Alkylresorcinol Metabolites in Urine by HPLC with Coulometric Electrode Array Detection, *Anja Koskela,¹ Anna-Maria Linko-Parvinen,^{1*} Perttu Hiisivuori,^{1,2} Adile Samaletdin,¹ Afaf Kamal-Eldin,³ Matti J. Tikkanen,^{1,2} and Herman Adlercreutz¹* (¹ Institute for Preventive Medicine, Nutrition and Cancer, Folkhälsan Research Center and Division of Clinical Chemistry, University of Helsinki, Helsinki, Finland; ² Department of Medicine, University of Helsinki, Helsinki, Finland; ³ Department of Food Science, Swedish University of Agricultural Science (SLU), Uppsala, Sweden; * Address correspondence to this author at: Institute for Preventive Medicine, Nutrition and Cancer, Folkhälsan Research Center and Division of Clinical Chemistry, PO Box 63, FIN-00014 University of Helsinki, Finland; fax 358-9-19125452, e-mail anna.linko@helsinki.fi)

Background: Whole-grain rye and wheat cereals contain high amounts of alkylresorcinols (ARs), phenolic lipids. ARs can be quantified in plasma. Two recently identified urinary AR metabolites, 3,5-dihydroxyphenylbenzoic acid (DHBA) and 3-(3,5-dihydroxyphenyl)-1-pro-

panoic acid (DHPPA), may be useful as biomarkers of intake of whole-grain rye and wheat.

Methods: We evaluated 4 pretreatment protocols for quantifying urinary DHBA and DHPPA using HPLC coupled with a coulometric electrode array detector. Syringic acid was used as the internal calibrator.

Results: Measured urinary concentrations of DHBA and DHPPA were 0.8–115 $\mu\text{mol/L}$. The mean recoveries of all added concentrations were 85%–104% for DHBA and 86%–99% for DHPPA, depending on the degree of the purification. The protocol versions with less purification correlated well with the protocol including highest purification. The correlation coefficients (r^2) were 0.9699–0.8153 for DHBA and 0.9854–0.8371 for DHPPA.

Conclusion: Although the protocol with the most purification steps was most specific, all protocols were suitable for measuring DHBA and DHPPA in urine. The rapid protocol with simple hydrolysis could be used in large-scale clinical studies. Additional investigation is needed to clarify whether these metabolites are useful biomarkers of whole-grain intake and helpful in the exploration of its association with human diseases.

© 2007 American Association for Clinical Chemistry

Epidemiological studies indicate that the consumption of whole-grain cereal products is beneficial, possessing health-promoting effects and decreasing the risk of several chronic diseases (1,2). Partly owing to a lack of reliable biomarkers, investigation of the association of whole-grain intake with disease prevalence has been difficult. Alkylresorcinols (ARs) are found in high concentrations in rye and wheat whole-grain cereals and have been proposed to function as plasma markers of whole-grain intake (3–5). ARs are absorbed via the lymphatic system and have a rather short elimination half-life (6,7). According to Ross et al. (8) the urinary secretion of intact ARs is minor. The urinary metabolites identified as 3,5-dihydroxybenzoic acid (DHBA) and 3-(3,5-dihydroxyphenyl)-1-propanoic acid (DHPPA) (8) were suggested by these authors to function as biological markers of whole-grain intake in humans. We describe a method for quantification of these metabolites in human urine.

We purchased acetonitrile, ethyl acetate, and methanol from Rathburn Chemicals; ortho-phosphoric acid from Riedel-de Haën; acetic acid, formic acid, potassium dihydrogenphosphate, and sodium acetate from Merck; syringic acid (SyrA), and sulfatase from Sigma-Aldrich; β -glucuronidase from Fluka; DHBA from Aldrich; and DHPPA from IsoSep AB.

We obtained 30 urine samples from 15 volunteers who consumed whole-grain wheat or rye bread for 1-week periods (9) and 3 urine samples from 3 volunteers with celiac disease who consumed no wheat or rye products. The Ethics Committee of the Department of Medicine, Helsinki University Central Hospital, Helsinki, Finland approved the study. All study participants gave informed

consent before the study, and gave permission to publish the results.

We used an HPLC system (ESA Biosciences) equipped with a model 540 autosampler, 2 model 580 solvent pumps, and a model 5600 coulometric electrode array detector (CEAD) with 8 electrode pairs. DHBA was quantified at 670 mV, DHPPA at 570 mV, and SyrA at 380 mV.

The analytes were separated using mobile phases consisting of 50 mmol/L phosphate buffer pH 2.3/methanol 90/10 (by volume) (phase A), and 50 mmol/L phosphate buffer pH 2.3/methanol/acetonitrile 40/40/20 (by volume) (phase B), with a 25-min linear gradient from 0% to 100% phase B (see Fig. 1 in the Data Supplement that accompanies the online version of this article at <http://www.clinchem.org/content/vol53/issue7>). The analytical column was an Inertsil ODS-3 (GL Sciences) 3 × 150 mm, connected to a Quick Release RP-18 (Upchurch Scientific) 3 × 10 mm guard column. Retention times, retention time variation, detection potentials, and detector response variation are presented in Table 1 in the online Data Supplement.

We developed sample preparation protocol C, with the highest amount of purification, and tested 3 modified protocols (A, B, and D) with different degrees of sample purification (Fig. 1).

To 100 μ L of urine we added 600 ng of internal calibrator SyrA in 8 μ L of methanol. The sample was hydrolyzed overnight at 37 °C with equal volume (100 μ L) of hydrolysis solution containing 0.1 mol/L Na-

acetate buffer pH 5, 0.2 kU/L β -glucuronidase, and 2 kU/L sulfatase. After incubation, 3 50- μ L aliquots A, B, and C (equal to 25 μ L of urine) were removed and treated as follows (aliquots A–C correspond to the protocols A–C):

For protocol A, 50 μ L each of methanol and HPLC mobile phase 20% phase B/phase A were added to the sample and then analyzed with HPLC-CEAD.

For protocol B, 500 μ L of methanol was added to the sample, and further purified using DEAE-Sephadex ion-exchange chromatography in the free base form (10). The sample was applied to the column with 500 μ L of methanol. Neutral steroids were eluted with 6 mL of methanol and discarded. DHBA and DHPPA were eluted with 8 mL of 0.5 mol/L formic acid in methanol. The fraction was evaporated, reconstituted with 50 μ L of methanol, 100 μ L of HPLC mobile phase 20% phase B/phase A was added, and the sample was analyzed with HPLC-CEAD.

For protocol C, a 50 μ L aliquot was extracted twice with 300 μ L of ethyl acetate. The combined organic phase was evaporated, reconstituted with 500 μ L of methanol, and further purified as described for protocol B.

For protocol D we added 60 μ L of methanol and 120 μ L of HPLC mobile phase 20% phase B/phase A to 20 μ L of nonhydrolyzed urine, and analyzed the sample directly with HPLC-CEAD.

For all 4 protocols (A–D) 10 μ L of the sample was injected into HPLC.

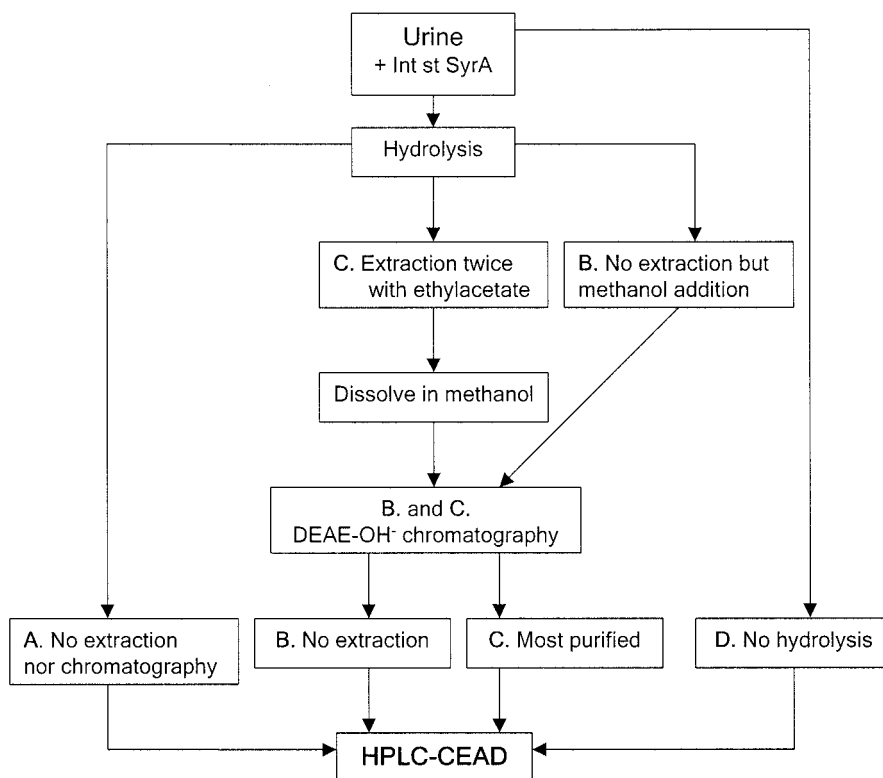


Fig. 1. Sample treatment protocols for urinary DHBA and DHPPA.

To test if deconjugation of the metabolites occurs during standing in the acidic environment before injection, we diluted urine followed by immediate injection. Nine additional injections from the same vial were performed during the following 8 h.

We measured the recoveries of DHBA and DHPPA in triplicate by supplementing 5 different concentrations of both compounds into low endogenous concentration urine samples. To avoid interference with the enzymatic hydrolysis from too high concentration of methanol, the added solutions were evaporated to dryness and reconstituted with a few microliters of methanol before addition of the urine. Six-point calibration curves (20–670 $\mu\text{g/L}$) were used. The mean recoveries of all added concentrations were 85%–104% for DHBA and 86%–99% for DHPPA, depending on the protocol used. Sample treatment protocol C yielded the lowest recoveries (see Table 2 in the online Data Supplement).

Reference calibrators were used to calculate limits of detection and to test the linearity. The limit of detection, using a signal:noise ratio of 3:1, and calculated as the amount of analyte per injection, was 5 pg/injection for both analytes. The limit of quantification, using a signal:noise ratio of 10:1, varied from 28 to 80 pg for DHBA and from 20 to 70 pg for DHPPA per injection, depending on the treatment protocol used, and corresponding to urine concentrations 0.17–0.48 $\mu\text{mol/L}$ and 0.13–0.45 $\mu\text{mol/L}$, respectively. Protocol C, including highest purification, gave the lowest limit of quantification. Linearity ranged from the limit of detection to 20 000 pg per injection for both analytes (the upper limit not tested), with correlation coefficients of 0.9990 for DHBA and 0.9994 for DHPPA.

Imprecision (Table 1) was evaluated by measuring 10 replicate control samples with 3 different concentrations in a single analysis (intraassay), and during 5 separate occasions (interassay).

The specificity of the method was based on the retention times and the oxidation patterns compared with

DHBA, DHPPA, and SyrA. Eleven other phenolic acids were tested: 3,4-dihydroxyphenylacetic acid, 3,4-dihydroxyphenylpropionic acid, 4-hydroxy,3-methoxymandelic acid, 4-hydroxyphenyl,2-propionic acid, caffeic acid, o-coumaric acid, m-coumaric acid, p-coumaric acid, ferulic acid, tannic acid, and sinapic acid. None had similar retention times and oxidation patterns.

All urine samples ($n = 33$) were quantified with all protocol versions. The quantitative results of samples analyzed with protocols A and B showed good correlations with the sample results of protocol C, using the highest purification (see Fig. 2 in the online Data Supplement). The correlation data for protocol D showed a slope of 0.74 for DHPPA, which we presume resulted from the lack of sample hydrolysis in protocol D, whereby the possible conjugates were not measured.

After 10 injections of diluted urine (protocol D) from the same sample vial, as described earlier, no change in DHPPA concentration was observed. The measured DHBA concentration, however, increased 15% within the first 2 h, possibly because of initial deconjugation, after which no change was observed (see Fig. 3 in the online Data Supplement). In all analysis sequences, 1 blank and 1 calibrator were placed first (total run time ~ 2 h), so all samples were waiting at least for 2 h before injection. Therefore no further change in DHBA concentrations in the analyzed samples occurred, and the results did not depend on what position in the sequence they were located.

The calibration linearity was greater than the concentrations of any of the samples analyzed, and we assumed that the linearity was sufficient for most normal urine samples. Protocol C was first chosen to get rid of the possible interfering compounds. When DHBA and DHPPA were found to occur in higher than anticipated concentrations, protocols A, and B, with less purification, were tested, as well as simple dilution of the urine (protocol D). The results using protocol D indicated that

Table 1. Intra- and interassay imprecision, with 3 control sample concentrations.^a

	Protocol A	Protocol B	Protocol C	Protocol D
DHBA^a	Straight from hydrolysis	No extraction	Most purified	Direct urine dilution
Low	4.1 (0.4)	2.4 (0.5)	1.0 (0.2)	4.1 (0.7)
Intra-/interassay CV %	3.6/8.8	12.5/21.8	9.5/16.7	7.1/15.9
Medium	15.9 (1.8)	15.9 (1.8)	14.1 (1.0)	13.9 (1.5)
Intra-/interassay CV %	3.4/11.2	6.5/11.1	4.7/7.4	7.8/10.9
High	34.7 (4.4)	36.9 (3.2)	32.6 (2.5)	46.4 (4.8)
Intra-/interassay CV %	9.7/12.7	4.2/8.5	3.3/7.7	5.3/10.3
DHPPA^a				
Low	8.0 (1.1)	6.2 (0.7)	5.7 (0.6)	8.0 (1.0)
Intra-/interassay CV %	1.5/13.2	5.7/11.5	4.4/10.1	3.5/12.4
Medium	23.2 (2.4)	23.4 (2.0)	23.0 (2.0)	15.1 (1.7)
Intra-/interassay CV %	2.5/10.1	4.2/8.5	6.0/8.7	8.3/11.6
High	40.4 (3.2)	44.5 (3.8)	43.3 (4.1)	26.3 (2.9)
Intra-/interassay CV %	11.1/7.9	4.9/8.5	6.7/9.5	5.9/11.1

^a Values are expressed as mean (SD) $\mu\text{mol/L}$. Intraassay ($n = 10$), interassay ($n = 5$).

DHBA and DHPPA mainly exist in the unconjugated form in urine. The protocols A, B, and C correlated well with each other (see Fig. 2 in the online Data Supplement), yielding similar results. Low concentrations (<7.1 $\mu\text{mol/L}$) of DHBA and DHPPA were found in urine samples from the volunteers with celiac disease. Gluten-free cereals, such as corn, millet, rice, and buckwheat, in addition to nuts and some varieties of peas, have a central role in the diets of patients with celiac disease. The low urinary concentrations of DHBA and DHPPA found in the celiac patients may be attributable to intake of millet, corn, cashew nuts, and garden pea varieties reported to contain minute amounts of ARs (3, 11, 12). Other dietary sources for minor formation of DHBA and DHPPA may be flavonoids (13), although these form mainly monohydroxylated and 2,3-, 2,4- or 3,4-dihydroxylated metabolites (14–16). The formation of 3,5-DHBA and 3,5-DHPPA metabolites is also possible. Further investigations are needed to find out if DHBA and DHPPA could be used as biomarkers of whole-grain intake.

Grant/funding support: We acknowledge the funding support received from Sigrid Jusélius Foundation, Ida Montin Foundation, Maud Kuistila Memorial Foundation, Finska Läkaresällskapet, and FORMAS. Vaasan & Vaasan Oy (Finland) provided the test breads used in the study. None of the authors had a conflict of interest regarding this study.

Financial disclosures: None declared.

Acknowledgments: We thank Prof. Per Åman, Swedish University of Agricultural Sciences, Uppsala, Sweden, for providing us with the reference calibrators DHBA and DHPPA.

References

- Seal CJ. Whole grains and CVD risk. *Proc Nutr Soc* 2006;65:24–34.
- Slavin J. Whole grains and human health. *Nutr Res Rev* 2004;17:99–110.
- Ross AB, Kamal-Eldin A, Åman P. Dietary alkylresorcinols: absorption, bioactivities, and possible use as biomarkers of whole-grain wheat- and rye-rich foods. *Nutr Rev* 2004;62:81–95.
- Linko A-M, Juntunen KS, Mykkänen HM, Adlercreutz H. Whole-grain rye bread consumption by women correlates with plasma alkylresorcinols and increases their concentration compared with low-fiber wheat bread. *J Nutr* 2005;135:580–3.
- Linko A-M, Parikka K, Wähälä K, Adlercreutz H. Gas chromatographic-mass spectrometric method for the determination of alkylresorcinols in human plasma. *Anal Biochem* 2002;308:307–13.
- Linko A-M, Ross AB, Kamal-Eldin A, Serena A, Bjørnbak Kjær AK, Jørgensen H, et al. Kinetics of the appearance of cereal alkylresorcinols in pig plasma. *Br J of Nutr* 2006;95:282–7.
- Landberg R, Linko A-M, Kamal-Eldin A, Vessby B, Adlercreutz H, Åman P. Human plasma kinetics and relative bioavailability of alkylresorcinols after intake of rye bran. *J Nutr* 2006;136:1–6.
- Ross AB, Åman P, Kamal-Eldin A. Identification of cereal alkylresorcinol metabolites in human urine-potential biomarkers of wholegrain wheat and rye intake. *J Chromatogr B Analyt Technol Biomed Life Sci* 2004;809:125–30.
- Linko-Parvinen A-M. Cereal alkylresorcinols as dietary biomarkers - absorption and occurrence in biological membranes. Helsinki: University of Helsinki, 2006.
- Fotsis T. The multicomponent analysis of estrogens in urine by ion exchange chromatography and GC-MS-II: fractionation and quantitation of the main groups of estrogen conjugates. *J Steroid Biochem* 1987;28:215–26.
- da Cruz Francisco J, Danielsson B, Kozubek A, Szwajcer Dey E. Application of supercritical carbon dioxide for the extraction of alkylresorcinols from rye bran. *J of Supercritical Fluids* 2005;35:220–6.
- Kubo I, Komatsu S, Ochi M. Molluscicides from the cashew *Anacardium occidentale* and their large-scale isolation. *J Agric Food Chem* 1986;34:970–3.
- Griffiths LA, Smith GE. Metabolism of myricetin and related compounds in the rat: metabolite formation in vivo and by intestinal microflora in vitro. *Biochem J* 1972;130:141–51.
- Makris DP, Rossiter JT. Comparison of quercetin and a non-orthohydroxy flavonol as antioxidants by competing in vitro oxidation reactions. *J Agric Food Chem* 2001;49:3370–7.
- Bode HB, Müller R. Possibility of bacterial recruitment of plant genes associated with the biosynthesis of secondary metabolites. *Plant Physiol* 2003;132:1153–61.
- Rios LY, Gonthier M-P, Rémésy C, Mila I, Lapiere C, Lazarus SA, et al. Chocolate intake increases urinary excretion of polyphenol-derived phenolic acids in healthy human subjects. *Am J Clin Nutr* 2003;77:912–8.

Previously published online at DOI: 10.1373/clinchem.2006.084764
